RECENT BaBar RESULTS ON HADRON SPECTROSCOPY*

Enrico Robutti

I.N.F.N. Genova
Via Dodecaneso 33, Genova, Italy

representing the BaBar Collaboration

(Received June 14, 2005)

Recent results from on hadronic spectroscopy are presented, based on data collected by the BaBar experiment between 1999 and 2004. The properties of the recently discovered $D^*_{sJ}(2317)^+$ and $D_{sJ}(2460)^+$ states are studied: resonance parameters and ratios of decay rates are measured from continuum e^+e^- production, and production rates are measured from B decays. A search for the $D^*_{sJ}(2632)^+$ state whose observation has been recently reported by the SELEX Collaboration, and a search for a charged partner of the charmonium-like $X(3872)$ state, are performed, yielding negative results. Finally, extensive searches for several pentaquark candidates, both fully inclusive and in B decays, result in no positive evidence.

PACS numbers: 13.66.Bc, 13.85.Ni, 13.85.Rm, 14.40.Gx

1. Introduction

The BaBar experiment [1], located at the PEP-II asymmetric e^+e^- collider at SLAC, has been taking data at the energy of the $\Upsilon(4S)$ since 1999. The large data samples recorded since then allow the carrying out of a large number of studies in the field of hadronic spectroscopy. States of interest are produced through a variety of mechanisms, including B decays, e^+e^- interactions, $\gamma\gamma$ fusion, initial state radiation (ISR) events. Studies on the properties of known states can be performed, as well as searches for new ones.

* Presented at the Cracow Epiphany Conference on Hadron Spectroscopy, Cracow, Poland, January 6–8, 2005.

This contribution reports recent results on the study of new states in the charmed strange mesons sector, of the charmonium-like $X(3872)$ state, and of pentaquark candidates. Results are based on different subsamples of the whole BaBar data sample at the end of 2004, corresponding to an integrated luminosity of about 250 fb^{-1}.

2. Properties of the new charmed strange mesons

The recent discovery [2, 3] of two new states, and the claim for a third one [4] in the charmed strange mesons sector has triggered considerable interest in the field, especially since the values of their masses and widths makes it difficult to accommodate them among the existing and predicted states [5] of the $c\overline{s}$ mesons [6] spectrum. For this reason, besides the favoured $c\overline{s}$ interpretation [7], alternative models have also been proposed [8, 9]. It is therefore of particular importance to acquire more information on their decay and production properties, and to get constraints on the value of their angular momentum.

2.1. $D^*_{sJ}(2317)^+$ and $D_{sJ}(2460)^+$ production in continuum e^+e^- interactions

The $D^*_{sJ}(2317)^+$ and $D_{sJ}(2460)^+$ states have been first observed by the BaBar and CLEO Collaborations [2, 3] in e^+e^- interactions through the decays $D^*_{sJ}(2317)^+ \to D^+_s\pi^0$ and $D_{sJ}(2460)^+ \to D^+_s\pi^0\gamma$, respectively. Subsequently, the Belle Collaboration has reported the observation of two other decay modes for the $D_{sJ}(2460)^+$: $D_{sJ}(2460)^+ \to D^+_s\gamma$ and $D_{sJ}(2460)^+ \to D^+_s\pi^+\pi^-$ [10]. BaBar has performed a study of all these decay modes on a sample of e^+e^- events corresponding to an integrated luminosity of 125 fb^{-1}.

A clean sample of D^+_s candidates is obtained by fitting to a common vertex a pair of oppositely charged kaons and a charged pion, and additionally requiring that either the $K^+\,K^-$ invariant mass be consistent with the ϕ mass, or the $K^-\,\pi^+$ invariant mass be consistent with the $K(892)$ mass: candidates whose $K^+\,K^-\,\pi^+$ invariant mass lies within 13.5 MeV of the D^+_s mass are then retained for further analysis.

The D^+_s candidates are combined with π^0 candidates and an unbinned maximum likelihood fit is performed on the resulting $D^+_s\,\pi^0$ invariant mass distribution, shown in Fig. 1 (left). Four contributions are considered: a $D^*_{sJ}(2317)^+ \to D^+_s\pi^0$ signal component, a combinatorial background component and two contributions arising from reflections of the $D^*_s(2112)^+ \to D^+_s\gamma$ and $D_{sJ}(2460)^+ \to D^+_s\pi^0\gamma$ decays, where an extra random photon is picked up, or one is missed in the reconstruction, respectively. In particular, because of a kinematical coincidence, the latter component produces a peak close to the value of the $D^*_{sJ}(2317)^+$ mass. The shape and size of this

component and the signal shape are taken from simulated events and fixed in the fit, while all other parameters are left free to float. After inclusion of the systematic uncertainties, the fit yields

$$m(D_{sJ}^*(2317)^+) = (2318.9 \pm 0.3(\text{stat}) \pm 0.9(\text{syst}))\,\text{MeV}/c^2.$$

Similarly, D_s^+ candidates are combined with energetic photons, and a fit to the resulting $D_s^+\gamma$ invariant mass distribution, shown in Fig. 1 (right), is performed. Along with the signal $D_{sJ}(2460)^+ \to D_s^+\gamma$ and the combinatorial background components, three contributions from reflections are considered: one from $D_{sJ}^*(2317)^+ \to D_s^+\pi^0$, one from $D_{sJ}(2460)^+ \to D_s^+\pi^0\gamma$ and one from hypothetical $D_{sJ}^*(2317)^+ \to D_s^+\gamma$ decays. The lineshapes of all but the first of these, as well as the signal shape, are taken from simulated events. After inclusion of the systematic uncertainties, the fit yields

$$m(D_{sJ}(2460)^+) = (2457.2.9 \pm 1.6(\text{stat}) \pm 1.3(\text{syst}))\,\text{MeV}/c^2.$$

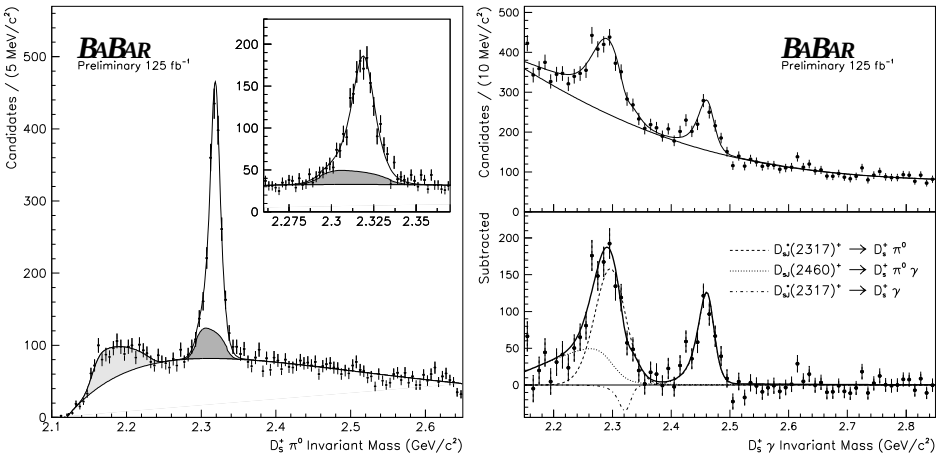

Fig. 1. Invariant mass distributions for combinations including D_s^+ candidates reconstructed in e^+e^- interactions. The solid curves show the results of unbinned maximum likelihood fits. Left: the D_s^+ π^0 invariant mass distribution for all selected candidates; the light (dark) shaded region represents the contribution from the ($D_{sJ}(2460)^+ \to D_s^+\pi^0\gamma$, $D_s^*(2112)^+ \to D_s^+\gamma$) reflection; the inset shows an expanded view around the $D_{sJ}^*(2317)^+$ mass. Right: the $D_s^+\gamma$ invariant mass for all selected candidates; in the lower plot the combinatorial contribution estimated by the fit is subtracted, and contributions from signal and reflections are shown in dashed lines.

The study of the $D_s^+\pi^0\gamma$ spectrum is then studied. In this case the $D_{sJ}(2460)^+ \to D_s^+\pi^0\gamma$ decay can be expected to proceed via the $D_{sJ}(2460)^+ \to D_s^*(2112)^+\pi^0$ or $D_{sJ}(2460)^+ \to D_{sJ}^*(2317)^+\gamma$ intermediate decay modes. However, the available phase space for the decay is such that the $D_s^+\gamma$ invariant mass must lie close to the $D_s^*(2112)^+$ mass in all cases. In order to separate the different components of signal and reflections, a fit is performed in three different regions of $m(D_s^+\gamma)$: one around the $D_s^*(2112)^+$ mass and two in upper and lower mass sidebands (Fig. 2 (left)). The reflections come from mis-reconstructed $D_s^*(2112)^+ \to D_s^+\gamma$ and $D_{sJ}^*(2317)^+ \to D_s^+\pi^0$ decays. The fit uses shapes derived from simulated events, and yields (after inclusion of the systematic uncertainties)

$$m(D_{sJ}(2460)^+) = (2459.1 \pm 1.3(\text{stat}) \pm 1.2(\text{syst}))\,\text{MeV}/c^2.$$

In order to disentangle the contributions from $D_{sJ}(2460)^+ \to D_s^*(2112)^+\pi^0$ and $D_{sJ}(2460)^+ \to D_{sJ}^*(2317)^+\gamma$, a second, two-dimensional unbinned likelihood fit to the $D_s^+\pi^0$ and $D_s^+\gamma$ invariant mass distributions is performed, with all possible contributions included. The results of this fit are consistent with the $D_{sJ}(2460)^+ \to D_s^+\pi^0\gamma$ proceeding entirely via $D_{sJ}(2460)^+ \to D_s^*(2112)^+\pi^0$.

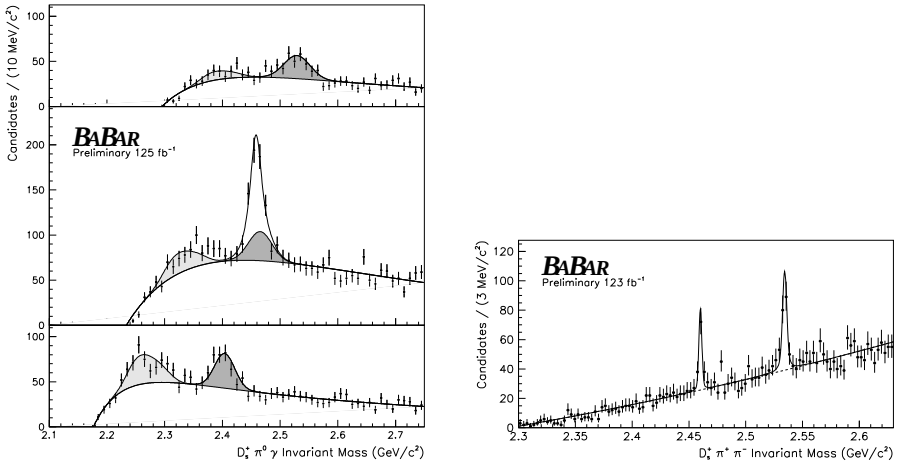

Fig. 2. Invariant mass distributions for combinations including D_s^+ candidates reconstructed in e^+e^- interactions. The solid curves show the results of unbinned maximum likelihood fits. Left: the $D_s^+\pi^0\gamma$ invariant mass distribution for selected candidates in the signal region (center) and in the $D_s^+\gamma$ high mass (top) and low mass (bottom) sidebands; the light (dark) shaded region represents the contribution from the $D_s^*(2112)^+ \to D_s^+\gamma$ ($D_{sJ}^*(2317)^+ \to D_s^+\pi^0$) reflection. Right: the $D_s^+\pi^+\pi^-$ invariant mass for all selected candidates.

Finally, the $D_s^+\,\pi^+\,\pi^-$ spectrum is studied. The invariant mass distribution, shown in Fig. 2 (right), is fitted to the sum of three signal components for the $D_{sJ}^*(2317)^+$, $D_{sJ}(2460)^+$, $D_{s1}(2536)^+$ states, plus a combinatorial background component. Signal shapes are determined from simulated events. The fit finds significant signals for $D_{sJ}(2460)^+$ and $D_{s1}(2536)^+$, and gives for their masses the values (after inclusion of the systematic uncertainties)

$$m(D_{sJ}(2460)^+) = (2460.1 \pm 0.3(\text{stat}) \pm 1.2(\text{syst}))\,\text{MeV}/c^2,$$

$$m(D_{s1}(2536)^+) = (2534.3 \pm 0.4(\text{stat}) \pm 1.2(\text{syst}))\,\text{MeV}/c^2.$$

Combining all results for the $D_{sJ}(2460)^+$ mass yields

$$m(D_{sJ}(2460)^+) = (2459.4 \pm 0.3(\text{stat}) \pm 1.0(\text{syst}))\,\text{MeV}/c^2.$$

Moreover, ratios of decay branching fractions for the $D_{sJ}(2460)^+$ can be calculated:

$$\frac{\mathcal{B}(D_{sJ}(2460)^+ \to D_s^+\gamma)}{\mathcal{B}(D_{sJ}(2460)^+ \to D_s^+\pi^0\gamma)} = 0.375 \pm 0.054(\text{stat}) \pm 0.057(\text{syst}),$$

$$\frac{\mathcal{B}(D_{sJ}(2460)^+ \to D_s^+\pi^+\pi^-)}{\mathcal{B}(D_{sJ}(2460)^+ \to D_s^+\pi^0\gamma)} = 0.082 \pm 0.018(\text{stat}) \pm 0.011(\text{syst}).$$

For more details on this analysis, see [11].

2.2. $D_{sJ}^*(2317)^+$ and $D_{sJ}(2460)^+$ production in B decays

The Belle Collaboration first observed $D_{sJ}^*(2317)^+$ and $D_{sJ}(2460)^+$ production in $B \to D_{sJ}^{(*)+}\overline{D}$ decays [12]. BaBar has performed a similar study, looking for $B \to D_{sJ}^{(*)+}\overline{D}^{(*)}$ decays on a sample corresponding to an integrated luminosity of about 113 fb^{-1}.

$\overline{D}$ and D_s^+ mesons are reconstructed in the modes

$$\begin{aligned}
\overline{D}^0 &\to K^+\pi^-,\ K^+\pi^-\pi^0,\ K^+\pi^-\pi^+\pi^-, \quad D^- \to K^+\pi^-\pi^-, \\
D_s^+ &\to \phi\pi^+(\phi \to K^+K^-), \quad D_s^+ \to \overline{K}^{*0}K^+(\overline{K}^{*0} \to K^-\pi^+).
\end{aligned}$$

D^* and $D_s^*(2112)^+$ candidates are reconstructed in the decay modes $D^{*+} \to D^0\pi^+$, $D^{*0} \to D^0\pi^0$, $D^0\gamma$, $D_s^*(2112)^+ \to D_s^+\gamma$.

The selected pairs of $D_s^{(*)+}$ and $\overline{D}^{(*)}$ are then combined with a photon or π^0 to form a B candidate; a veto on events consistent with $B \to D_s^{(*)+}\overline{D}^{(*)}$ decays is applied. The B selection is based on a pair of kinematical variables:

the beam-energy-substituted mass, $m_{\rm ES} \equiv \sqrt{s/4 - {p^*_B}^2}$, and the difference between the reconstructed energy of the B candidate and the beam energy, $\Delta E \equiv E^*_B - \sqrt{s}/2$, where $\sqrt{s}$ is the total energy in the $\Upsilon(4S)$ center-of-mass frame and E^*_B (p^*_B) is the energy (momentum) of the B candidate in the same frame.

A signal region is defined in the $m_{\rm ES}$-ΔE plane: for each of the twelve modes considered, the signal yield is then determined from fits to the $D_s^+\pi^0$ (for $D^*_{sJ}(2317)^+$), and $D_s^*(2112)^+\pi^0$, $D_s^+\gamma$ (for $D_{sJ}(2460)^+$) invariant mass distributions for events in the $m_{\rm ES}$-ΔE signal region. The fits include a Gaussian signal and a smooth background component. Cross-feed contributions between different $D^{(*)+}_{sJ}$ decay modes are taken into account. The resulting branching fractions, after including systematic uncertainties, are listed in Table I. A significant signal is seen in nearly all modes; in particular, the D^* modes are observed for the first time.

TABLE I

Branching fractions and signal significance for $B \to D^{(*)+}_{sJ}\overline{D}^{(*)}$ decays. The first error on $\mathcal{B}$ is statistical, the second is systematic, the third is from the $\overline{D}$ and D_s^+ branching fractions.

B mode		$\mathcal{B}(10^{-3})$	Significance
$B^0 \to D^*_{sJ}(2317)^+ D^-$	$[D_s^+\pi^0]$	$1.8 \pm 0.4 \pm 0.3^{+0.6}_{-0.4}$	5.5
$B^0 \to D^*_{sJ}(2317)^+ D^{*-}$	$[D_s^+\pi^0]$	$1.5 \pm 0.4 \pm 0.2^{+0.5}_{-0.3}$	5.2
$B^+ \to D^*_{sJ}(2317)^+ \overline{D}^0$	$[D_s^+\pi^0]$	$1.0 \pm 0.3 \pm 0.1^{+0.4}_{-0.2}$	3.1
$B^+ \to D^*_{sJ}(2317)^+ \overline{D}^{*0}$	$[D_s^+\pi^0]$	$0.9 \pm 0.6 \pm 0.2^{+0.3}_{-0.2}$	2.5
$B^0 \to D_{sJ}(2460)^+ D^-$	$[D_s^{*+}\pi^0]$	$2.8 \pm 0.8 \pm 0.5^{+1.0}_{-0.6}$	4.2
$B^0 \to D_{sJ}(2460)^+ D^{*-}$	$[D_s^{*+}\pi^0]$	$5.5 \pm 1.2 \pm 1.0^{+1.9}_{-1.2}$	7.4
$B^+ \to D_{sJ}(2460)^+ \overline{D}^0$	$[D_s^{*+}\pi^0]$	$2.7 \pm 0.7 \pm 0.5^{+0.9}_{-0.6}$	5.1
$B^+ \to D_{sJ}(2460)^+ \overline{D}^{*0}$	$[D_s^{*+}\pi^0]$	$7.6 \pm 1.7 \pm 1.8^{+2.6}_{-1.6}$	7.7
$B^0 \to D_{sJ}(2460)^+ D^-$	$[D_s^+\gamma]$	$0.8 \pm 0.2 \pm 0.1^{+0.3}_{-0.2}$	5.0
$B^0 \to D_{sJ}(2460)^+ D^{*-}$	$[D_s^+\gamma]$	$2.3 \pm 0.3 \pm 0.3^{+0.8}_{-0.5}$	11.7
$B^+ \to D_{sJ}(2460)^+ \overline{D}^0$	$[D_s^+\gamma]$	$0.6 \pm 0.2 \pm 0.1^{+0.2}_{-0.1}$	4.3
$B^+ \to D_{sJ}(2460)^+ \overline{D}^{*0}$	$[D_s^+\gamma]$	$1.4 \pm 0.4 \pm 0.3^{+0.5}_{-0.3}$	6.0

From the measured branching fractions for $B \to D_{sJ}(2460)^+\overline{D}^{(*)}$ in the $D_s^*(2112)^+\pi^0$ and in the $D_s^+\gamma$ final states, one gets the ratio

$$\frac{\mathcal{B}(D_{sJ}(2460)^+ \to D_s^+\gamma)}{\mathcal{B}(D_{sJ}(2460)^+ \to D_s^*(2112)^+\pi^0)} = 0.274 \pm 0.045(\text{stat}) \pm 0.020(\text{syst}).$$

A helicity analysis of the $D_{sJ}(2460)^+$ state is performed using the decays $B^+ \to D_{sJ}(2460)^+\overline{D}^0$ and $B^0 \to D_{sJ}(2460)^+D^-$, with $D_{sJ}(2460)^+ \to D_s^+\gamma$. The helicity angle θ_h is defined as the angle between the D_s^+ and the parent B momenta in the $D_{sJ}(2460)^+$ rest frame: fits to $m(D_s^+\gamma)$ are performed for five different $\cos(\theta_h)$ regions. The resulting angular distribution is shown in Fig. 3: it is in good agreement with the $J = 1$ hypothesis, while the $J = 2$ hypothesis is excluded. For more details on this analysis, see [13].

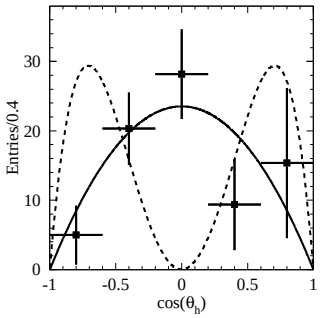

Fig. 3. The helicity distribution for $B \to D_{sJ}(2460)^+D$, $D_{sJ}(2460)^+ \to D_s^+\gamma$ events, obtained from fits to $m(D_s^+\gamma)$ in different bins of $\cos(\theta_h)$. The solid (dashed) line shows the expected distribution for a $J = 1$ ($J = 2$) $D_{sJ}(2460)^+$ state.

2.3. Search for the $D_{sJ}^*(2632)^+$ state

The SELEX Collaboration has recently reported evidence for the existence of a narrow state at a mass of 2632 MeV/c^2 decaying to $D_s^+\eta$ and D^0K^+ [4]. Using $D^{(*)}$ and D_s^+ mesons produced in e^+e^- interactions from a sample corresponding to an integrated luminosity of 125 fb^{-1}, BaBar has searched for evidence of resonant structures in this mass region.

D_s^+ mesons are reconstructed as described in Sec. 2.1; η mesons are reconstructed from photon pairs, with the requirement that they do not overlap with π^0 or $D_s^*(2112)^+ \to D_s^+\gamma$ candidates. The $D_s^+\eta$ invariant mass spectrum is studied by subtracting background contributions from $m(K^+K^-\pi^+)$ and $m(\gamma\gamma)$ sidebands from the spectrum observed in the $m(D_s^+)$–$m(\eta)$ region. The resulting distribution is shown in Fig. 4 (left): there is no evidence for enhancements around 2632 MeV/c^2.

The D^0K^+ mass spectrum is investigated using the $D^0 \to K^-\pi^+$ decay mode. The invariant mass distribution resulting from pairing reconstructed D^0 mesons with charged kaons is shown in Fig. 4 (center): a clear peak is seen at the mass of the $D_{s2}(2573)^+$ state, but no other structure is visible.

Finally, D^{*+} mesons are reconstructed from a D^0 and a charged pion, requiring that the mass difference $m(D^0\pi^+) - m(D^0)$ be consistent with that

for a D^{*+}, and combined with K^0_S candidates reconstructed from pairs of oppositely charged pions. The mass difference distribution $m(D^{*+}K^0_S) - m(D^{*+})$ is shown in Fig. 4 (right): a large peak corresponding to the $D_{s1}(2536)^+$ state is visible, but again no evidence is found for structures around 2632 MeV/c^2. For more details on this analysis, see [14].

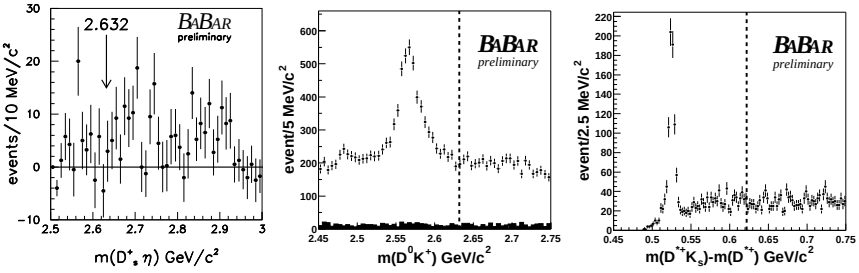

Fig. 4. The $D_s^+\eta$ (left), D^0K^+ (center), $D^{*+}K^0_S$ (right) invariant mass distributions for selected candidates in e^+e^- interactions. The arrow and dashed lines indicate the position where a $D^*_{sJ}(2632)^+$ signal should appear.

3. The $X(3872)$ state

Since the discovery of the $X(3872)$ state, observed by the Belle Collaboration [15] in the $J/\psi\ \pi^+\ \pi^-$ spectrum in B decays, several confirmations, from CDF [16], D0 [17] and BaBar [18] have appeared. Nevertheless, the true nature of this state is still not understood, and the "natural" assignment to a charmonium state is put in doubt by several observations disfavouring all specific quantum number assignments [19]. Several other interpretations have been proposed, including a D^*D bound state [20], a hybrid charmonium state [21], a diquark–antidiquark state [9].

3.1. Search for a charged partner

The invariant mass distribution of the dipion system in $X(3872) \to J/\psi\,\pi^+\pi^-$ decays has been shown to peak close to its upper kinematic limit, and is consistent with a $X(3872) \to J/\psi\,\rho^0$ decay. If this were the case, and if the decay were isospin-conserving, then the $X(3872)$ would be an isovector state, and a charged $X(3872)^-$ partner should exist, decaying to $J/\psi\,\pi^-\pi^0$. A search for such a state has been conducted by BaBar in B meson decays from a sample corresponding to an integrated luminosity of 212 fb^{-1}.

The search is performed in the neutral $B^0 \to J/\psi\,\pi^-\pi^0K^+$ and charged $B^- \to J/\psi\,\pi^-\pi^0K^0_S$ decay modes. J/ψ are reconstructed from e^+e^- and $\mu^+\mu^-$ pairs, K^0_S from $\pi^+\ \pi^-$ pairs. The B candidate selection relies on the $m_{\rm ES}$ and ΔE variables.

The $J/\psi\ \pi^-\ \pi^0$ invariant mass distribution for candidates lying in a signal region defined in the $m_{\rm ES}$-ΔE plane is shown in Fig. 5 for the neutral (left) and charged (right) mode. No peaks are seen around 3872 MeV/c^2. Upper limits for the production rates are extracted after estimating the contributions from combinatorial background and non-resonant B decays in the $X(3872)$ mass region:

$$\mathcal{B}(B^0 \to X(3872)^- K^+, X(3872)^- \to J/\psi\pi^-\pi^0) < 5.4 \times 10^{-6}\ (90\%\text{CL})\,,$$

$$\mathcal{B}(B^- \to X(3872)^- \overline{K}^0, X(3872)^- \to J/\psi\pi^-\pi^0) < 22 \times 10^{-6}\ (90\%\text{CL})\,.$$

For more details on this analysis, see [22].

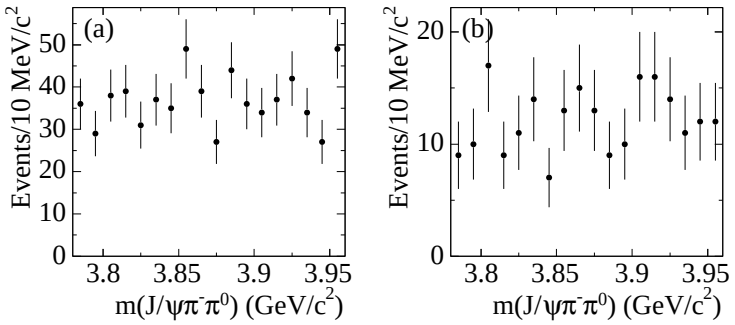

Fig. 5. The $J/\psi\pi^-\pi^0$ invariant mass distribution for reconstructed $B^0 \to J/\psi\pi^-\pi^0 K^+$ (left) and $B^- \to J/\psi\pi^-\pi^0 K^0_{\rm S}$ (right) events.

4. Pentaquark searches

A large number of experiments have recently reported evidence for peaks in invariant mass spectra of final states containing a baryon, whose quark content is not consistent with coming from the decay of a conventional hadronic state. In particular, more than 10 evidences have been reported for a narrow structure around 1540 MeV/c^2, in nK^+ or $pK^0_{\rm S}$ spectra; a single experiment (NA49) finds evidence for narrow peaks at 1862 MeV/c^2 in the $\Xi^-\pi^-$ and $\Xi^-\pi^+$ spectra; another single evidence (from H1) is reported for a narrow enhancement around 3100 MeV/c^2 in the $D^{*-}p$ spectrum. All these states can be considered as candidates for pentaquark states, composed of four quarks and an antiquark; they are commonly referred to as $\Theta(1540)^+$, $\Xi_5(1860)^{--}$, $\Xi_5(1860)^0$, $\Theta_c(3100)^0$. Several theoretical models [23] have been proposed to describe possible pentaquark structures.

On the other hand, a number of experiments that observe large samples of strange baryons with mass similar to that of the $\Theta(1540)^+$ see no evidence

for it; and a number of experiments that observe large samples of the non-exotic Ξ^- baryon do not observe the $\Xi_5(1860)^{--}$, $\Xi_5(1860)^0$ states. A fairly recent review of positive and negative results can be found in [24].

4.1. Inclusive searches for pentaquark candidates

BaBar has performed an inclusive search for $\Theta(1540)^+ \to pK^0_S$, $\Xi_5(1860)^{--} \to \Xi^-\pi^-$ and $\Xi_5(1860)^0 \to \Xi^-\pi^+$ on a data sample corresponding to 123 fb^{-1}.

K^0_S reconstructed from $\pi^+\,\pi^-$ pairs are combined with tracks identified as protons, with a vertex close to the interaction point. The pK^0_S invariant mass spectrum for these candidates is shown in Fig. 6 (top): a clear peak corresponding to the Λ_c^+ state is visible above a smooth background, but no enhancement is seen in the region of the $\Theta(1540)^+$.

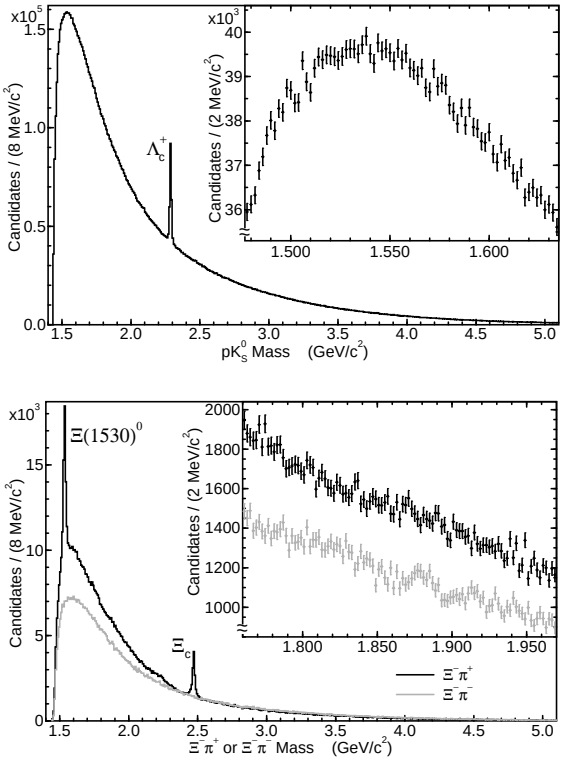

Fig. 6. Distribution of the pK^0_S (top) and $\Xi^-\pi^-$, $\Xi^-\pi^+$ (bottom) invariant mass for all selected combinations. The insets show expanded views of the regions where observations of the $\Theta(1540)^+$ (top) and $\Xi_5(1860)^{--}$, $\Xi_5(1860)^0$ (bottom) have been reported.

In order to increase the sensitivity to production mechanisms favouring certain momentum ranges, the sample is divided in 10 subsamples according to the center-of-mass momentum of the pK^0_S system, from 0 to 5 GeV. No evidence for a $\Theta(1540)^+$ candidate is found in any of the resulting spectra. Upper limits for the production cross section are calculated for each p^* bin, by means of a fit to the invariant mass spectrum, and assuming for $\Theta(1540)^+$ a total width equal to 1 MeV or to the current upper limit of 8 MeV. In the hypothesis that the $\Theta(1540)^+$ decays strongly, the decay branching fraction is assumed to be $\mathcal{B}(\Theta(1540)^+ \to pK^0_S) = 0.25$. These results are shown in the upper part of Fig. 7.

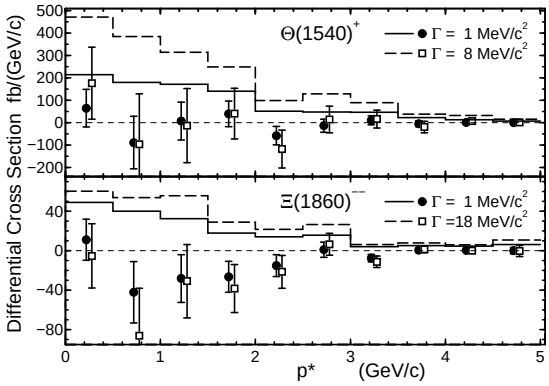

Fig. 7. The measured differential production cross sections (symbols) and corresponding 95% CL upper limits (lines) for $\Theta(1540)^+$ (top) and $\Xi_5(1860)^{--}$ (bottom), assuming natural widths of $\Gamma = 1\,\mathrm{MeV}$ (solid) and at the current experimental upper limit (dashed), as functions of the CM momentum.

Ξ^- baryons are reconstructed through the decay chain $\Xi^- \to \Lambda^0\pi^-$, $\Lambda^0 \to p\pi^-$. Particle identification, vertexing and flight distance requirements are applied. They are combined with charged tracks coming from the interaction vertex: the resulting $\Xi^-\pi^-$ and $\Xi^-\pi^+$ invariant mass spectra are shown in Fig.6. Again, clear peaks for the conventional $\Xi(1530)^0$ and $\Xi_c(2470)^0$ baryons can be seen in the $\Xi^-\pi^+$ spectrum, but no enhancement is found around 1860 MeV/c^2.

As for the $\Theta(1540)^+$, the sample is divided in 10 p^* bins, and upper limits to the production cross section are extracted in each of them from fits to the invariant mass distribution. The total width of the $\Xi_5(1860)^{--}$ state is fixed to 1 MeV or the current upper limit of 18 MeV. The decay branching fraction is assumed in this case to be $\mathcal{B}(\Xi_5(1860)^{--} \to \Xi^-\pi^-) = 0.5$. Results are shown in the lower part of Fig. 7. For more details on this analysis, see [25].

4.2. Searches in B decays

Following the observation of the $B^- \to p\overline{p}K^+$ decay [26], it has been suggested that this process might receive a contribution from $B^- \to \Theta^{*++}\overline{p}$, $\Theta^{*++} \to pK^+$, where Θ^{*++} would be a pentaquark member of the baryon 27-plet, predicted to lie in the region 1.43–1.70 GeV/c^2. Such a hypothesis has been tested by BaBar on a data sample corresponding to an integrated luminosity of 81 fb^{-1}.

B candidates are selected based on cuts on the $m_{\rm ES}$, ΔE kinematic variables and on shape variables used to reduce the large continuum background. The pK^+ invariant mass distribution for events in the signal region is shown in Fig. 8 up to 3.4 GeV/c^2. Out of the 212 selected events, none lies below 1.85 GeV/c^2. Upper limits for the product of branching ratios are calculated for different regions of $m(\Theta^{*++})$. For the range 1.43–1.85 GeV/c^2 one gets

$$\mathcal{B}(B^- \to \overline{p}\Theta^{*++}, \Theta^{*++} \to pK^+) < 1.5 \times 10^{-7}\ (90\%\text{CL})\,.$$

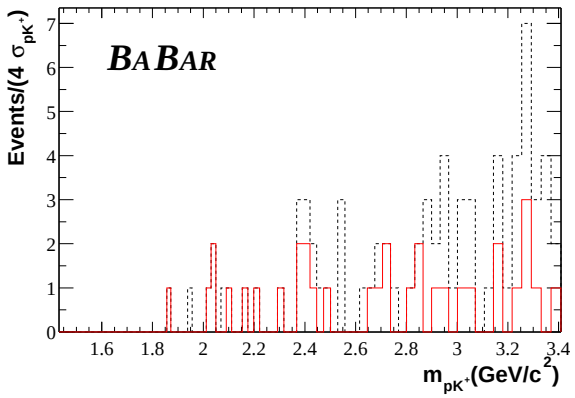

Fig. 8. The pK^+ invariant mass distribution for selected $B^- \to p\overline{p}K^+$ events in the charmonium region $2.85 < m(p\overline{p}) < 3.15\,\text{GeV}/c^2$ (solid line) and outside (dashed line).

The observation of $B^0 \to \overline{D}^{(*)}p\overline{p}$, $B^0 \to \overline{D}^{(*)}p\overline{p}\pi$ decays allows the search for resonant structures in the $D^{(*)}\,(\overline{p})$ invariant mass spectra. These would indicate the presence of heavy charmed baryons or charmed pentaquarks, such as the one observed by H1. BaBar has performed such a study on a data sample corresponding to an integrated luminosity of 113 fb^{-1}.

D candidates are reconstructed in the $D^- \to K^+\pi^-\pi^-$, $\overline{D}^0 \to K^+\pi^-$ decay modes; D^* candidates are reconstructed from $D^{*-} \to \overline{D}^0\pi^-$, $\overline{D}^{*0} \to \overline{D}^0\pi^0$. $m_{\rm ES}$ and ΔE are used to select B candidates.

Two of the eight $D^{(*)}$ $(\overline{p})$ resulting spectra are shown in Fig. 9: none of them shows evidence of significant peaking structures. For more details on these analyses, see [27] and [28].

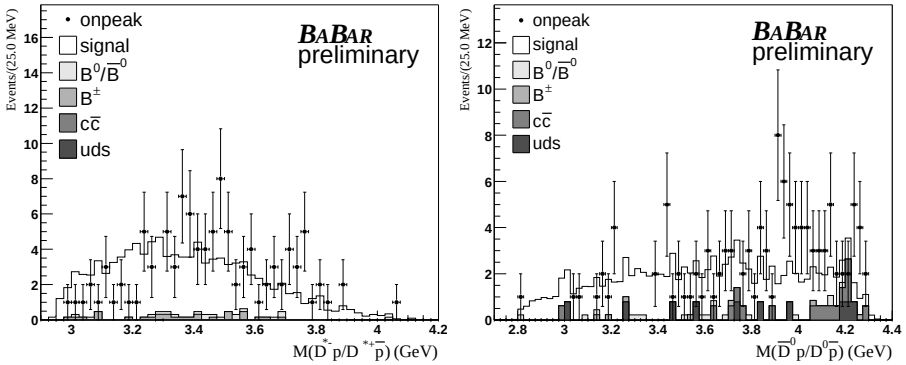

Fig. 9. The invariant mass distribution of $D^{*-}p$ (left) and $\overline{D}^0 p$ (right) combinations from signal candidates in the $B^0 \to D^{*-}p\overline{p}\pi^+$ (left) and $B^0 \to \overline{D}^0 p\overline{p}$ (right) decay mode. The cross-hatched histograms represent the contributions from different background sources; the open histogram is the expected contribution from phase-space signal simulation.

REFERENCES

[1] B. Aubert *et al.* (BaBar Collaboration), *Nucl. Instrum. Methods Phys. Res.* **A479**, 1 (2002).

[2] B. Aubert *et al.* (BaBar Collaboration), *Phys. Rev. Lett.* **90**, 90242001 (2003).

[3] D. Benson *et al.* (CLEO Collaboration), *Phys. Rev.* **D68**, 032002 (2003).

[4] A.V. Evdokimov *et al.* (SELEX Collaboration), *Phys. Rev. Lett.* **93**, 242001 (2004) [hep-ex/0406045].

[5] S. Godfrey, N. Isgur, *Phys. Rev.* **D32**, 189 (1985); S. Godfrey, R. Kokoski, *Phys. Rev.* **D43**, 1679 (1991); M. Di Pierro, E. Eichten, *Phys. Rev.* **D64**, 114004 (2001).

[6] Charge conjugate states are always implied, unless otherwise stated.

[7] R.N. Cahn, J.D. Jackson, *Phys. Rev.* **D68**, 037502 (2003); W.A. Bardeen, E.J. Eichten, C.T. Hill, *Phys. Rev.* **D68**, 054024 (2003); S. Godfrey, *Phys. Lett.* **B568**, 254 (2003); Y.B. Dai, C.S. Huang, C. Liu, S.L. Zhu, *Phys. Rev.* **D68**, 114011 (2003); A. Deandrea, G. Nardulli, A.D. Polosa, *Phys. Rev.* **D68**, 097501 (2003).

[8] T. Barnes, F.E. Close, H.J. Lipkin, *Phys. Rev.* **D68**, 054006 (2003); E. van Beveren, G. Rupp, *Phys. Rev. Lett.* **91**, 012003 (2003); H.Y. Cheng, W.S. Hou, *Phys. Lett.* **B566**, 193 (2003); A.P. Szczepaniak, *Phys. Lett.* **B567**, 23 (2003); T.E. Browder, S. Pakvasa, A.A. Petrov, *Phys. Lett.* **B578**, 365 (2004).

[9] L. Maiani *et al.*, *Phys. Rev.* **D71**, 014028 (2005).

[10] K. Abe *et al.* (Belle Collaboration), *Phys. Rev. Lett.* **92**, 012002 (2004).

[11] B. Aubert *et al.* (BaBar Collaboration), `hep-ex/0408067`.

[12] P. Krokovny *et al.* (Belle Collaboration), *Phys. Rev. Lett.* **91**, 262002 (2003).

[13] B. Aubert *et al.* (BaBar Collaboration), *Phys. Rev. Lett.* **93**, 181801 (2004).

[14] B. Aubert *et al.* (BaBar Collaboration), `hep-ex/0408087`.

[15] S.K. Choi *et al.* (Belle Collaboration), *Phys. Rev. Lett.* **91**, 262001 (2003).

[16] D. Acosta *et al.* (CDF Collaboration), *Phys. Rev. Lett.* **93**, 072001 (2004).

[17] V.M. Abazov *et al.* (D0 Collaboration), *Phys. Rev. Lett.* **93**, 162002 (2004).

[18] B. Aubert *et al.* (BaBar Collaboration), *Phys. Rev.* **D71**, 071103 (2005).

[19] K. Abe *et al.* (Belle Collaboration), `hep-ex/0408116`; S. Dobbs *et al.* (CLEO Collaboration), *Phys. Rev. Lett.* **94**, 032004 (2005).

[20] N. Tornqvist, *Phys. Lett.* **B590**, 209 (2004); M.B. Voloshin, *Phys. Lett.* **B579**, 316 (2004); F. Close, P. Page, *Phys. Lett.* **B578**, 119 (2004); C.Y. Wong, *Phys. Rev.* **C69**, 055202 (2004); E. Braaten, M. Kusunoki, *Phys. Rev.* **D69**, 074005 (2004); E. Swanson, *Phys. Lett.* **B588**, 189 (2004).

[21] F. Close, S. Godfrey, *Phys. Lett.* **B574**, 210 (2003).

[22] B. Aubert *et al.* (BaBar Collaboration), *Phys. Rev.* **D71**, 031501 (2005).

[23] D. Diakonov, V. Petrov, M.V. Polyakov, *Z. Phys.* **A359**, 305 (1997); M. Karliner, H. Lipkin, *Phys. Lett.* **B575**, 249 (2003); R. Jaffe, F. Wilczek, *Phys. Rev. Lett.* **91**, 232003 (2003).

[24] J. Pochodzalla, `hep-ex/0406077`, and references therein. See also other contributions to the Proceedings of this Conference.

[25] B. Aubert *et al.* (BaBar Collaboration), `hep-ex/0502004`, submitted to *Phys. Rev. Lett.*

[26] K. Abe *et al.* (Belle Collaboration), *Phys. Rev. Lett.* **88**, 181803 (2002).

[27] B. Aubert *et al.* (BaBar Collaboration), `hep-ex/0408037`.

[28] B. Aubert *et al.* (BaBar Collaboration), `hep-ex/0408035`.